# METHOD FOR CALCULATING OBSERVABILITY OF AIRCRAFT FLIGHT ROUTE

**Wang Xu, Song Bi Feng**
**School of Aeronautics, Northwestern Polytechnical University, Xi'an 710072, P. R. China**

**Keywords**: *aircraft flight route, probability of detection, radar cross section (RCS)*

## Abstract

*A method for calculating the observability of flight route in the presence of radar detection systems is proposed. The scenario of aircraft-radar system encounter is analyzed. The probability of detection of the aircraft near the radar system depends on aircraft radar cross section, flight route, and radar system configuration. The aircraft radar cross section model is based on the Kriging spatial prediction technique. The radar detection systems have a square law detector and a cell averaging constant false alarm rate (CA-CFAR) processor. The observability of aircraft flight route is represented by the cumulative probability of detection. The numerical simulations are used to illustrate the properties of the proposed method. This work will be useful for the low-observable aircraft flight route planning.*

## 1 Introduction

One of the main threats for combat aircraft is radar detection systems. Reducing the observability of aircraft in the presence of radar detection systems is one of the ways to the improvement of aircraft survivability. In general, the observability of aircraft can be reduced or decreased by 1) a good design that reduces the signature of aircraft; 2) the proper tactics of aircraft.

Recent investigations have showed that flight routes can significantly influence the observability of aircraft by radars [1, 2]. And low-observability trajectory planning has been studied by several investigators since 1999. Work by McFarland et al. [3] uses motion planning techniques using potential field theory for unmanned air vehicle path planning in the presence of detection systems. This is a technique originally used in robot motion planning. Moore [4] established a methodology for minimizing the peak and/or aggregate radar cross sections of autonomous precision guided munitions as they ingress to a selected target through a radar threat environment. Norsell [5] investigated the problem of finding an optimal aircraft trajectory subject to constraints defining distance of detection by a radar station. K. Misovec et al. [6, 7] studied the use of the nonlinear trajectory generation method as a solution to the low observability path planning challenge. Chaudhry et al. [8] described a method that uses Mixed Integer Linear Programming to the low observability path planning problem.

Although much work has been devoted to low observability path planning methods and each method would give one or more optimal flight routes, little work has been published on how these flight routes' observability is measured. The purpose of this paper is to propose a method for calculating observability of aircraft flight route.

This paper begins with an analysis of aircraft-radar system encounter scenario. Three most important models including the aircraft RCS, flight route and radar detection models are discussed. Then the calculation of observability of aircraft flight route is developed. To investigate the effectiveness of the proposed method, two numerical examples are considered. Finally, conclusions and future research directions are presented.

## 2 Aircraft-Radar System Encounter

Consider the aircraft and the radar system shown in Fig. 1. The aircraft flies into a geographical area, defended by threat radar system. The probability that the aircraft is detected by the radar system depends on three aspects, aircraft radar cross section, flight route and radar system configuration. We will give the detailed analyses of these three aspects in the following section.

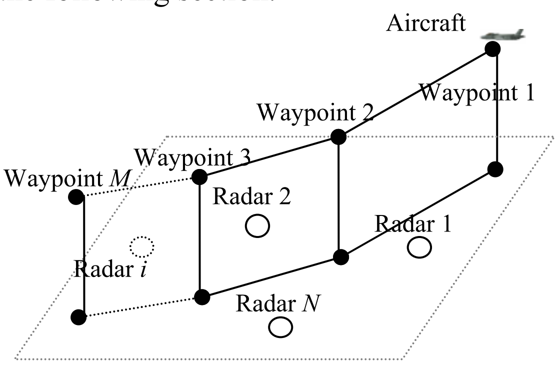


Fig. 1 Aircraft-Radar System Encounter

### 2.1 Aircraft RCS

RCS for an aircraft depends on the direction of the radiated signal and the direction of the receiving antenna. The radar polarization and radar wavelength are important when computing aircraft observability. The size and shape of an aircraft and the electromagnetic properties of its materials determine the magnitude of its RCS.

Although RCS for an aircraft can be predicted by computer programs or measured by experiments, the accurate prediction and measurement of the RCS of a specific aircraft as a function of viewing angle or aspect for a given radar are very difficult task [9]. Most of the time, the RCS values are known only at some given aspects. This is not suitable for the calculating observability of aircraft flight route, so the Kriging spatial prediction technique is used here. There is some computer power needed to determine the Kriging coefficients, but when this is done, the prediction of RCS at a certain viewing angle can be calculated very quickly. In the calculating of the observability of aircraft flight route, a lot of function evaluations including RCS calculation are performed which makes Kriging very suitable for this purpose.

When the aircraft is in motion, its aspect with respect to the radar is bound to vary by some small amount on every scan of the target, and this variation can cause a significant fluctuation in the magnitude of RCS seen by the radar, and this fluctuation has an important effect upon the probability the aircraft is detected. The 'Swerling' distribution models define several possible cases of RCS fluctuation. In this paper, It is assumed that at a specific viewing angle the aircraft RCS fluctuation model is 'Swerling-I' [10].

### 2.2 Flight Route

Assume the start waypoint of the aircraft flight route is ($x_s$, $y_s$, $z_s$), the target waypoint is ($x_t$, $y_t$, $z_t$), and ($x_i$, $y_i$, $z_i$) is the $i$-th waypoint, the flight route of the aircraft can be described by Fig. 2.

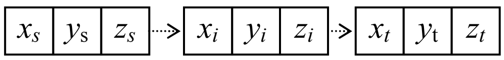


Fig. 2 Expression of Flight Path

Because our purpose is calculating the observability of aircraft flight route, we assume that the flight route is known in this paper.

### 2.3 Detection Models

Radar is the only threat against aircraft considered in this paper, and we assume that the radars are on the ground. This section gives the radar detection model. Assume the radar has a square law detector and a cell averaging constant false alarm rate (CA-CFAR) processor, the background is homogeneous Gaussian distribution, and the fluctuation model of target RCS is 'Swerling-I' distribution model, then the probability of detection $p_d$ and the probability of false alarm $p_{fa}$ is given by [11]

$$p_d = (1 + t/(1+S))^{-K} \quad (1)$$

$$p_{fa} = (1+t)^{-K} \quad (2)$$

where $K$ is the number of reference cells of the CA-CFAR processor, which is known for a given radar; $t$ is the constant scale factor; $S$ is the average signal-to-noise ratio (SNR).

The signal-to-noise ratio plays a major role in the detection capability of radar. From the radar equation, we know that the signal-to-noise ratio is a function of the target RCS (σ), the distance between the target and the radar antenna ($R$), and the radar system characteristics as [12]

$$S = \frac{P_r G_r^2 \lambda^2 \sigma F^4}{(4\pi)^3 L_S L_\alpha N R^4} \quad (3)$$

where $P_r$ is the radar power, $G_r$ is the gain of the antenna, λ is the radar wavelength, σ is the target radar cross section, $F$ is the pattern propagation factor, $L_a$ and $L_S$ are the atmospheric loss factor and radar system loss factor, respectively, $N$ is the noise power; $R$ is the distance between the target and the radar antenna.

The equation above can be split into two separate parts, one part is dependent on the radar systems consist of $P_r$, $G_r$, λ, $L_S$ and $N$, and the other part is dependent on the propagation path of the electromagnetic wave including $F$ and $L_a$., $\sigma$ and $R$. The first part is denoted as $v_0$, so Eq. (3) can be rewritten as

$$S = v_0 \frac{\sigma F^4}{R^4 L_\alpha} \quad (4)$$

where $v_0$ is constant for a given radar.

In order to calculate the probability that a target is detected by a given radar, we must know some basic system parameters of the radar. The detection ability of a radar is often described by maximum detection range $R_0$, which means that the radar can detect a target of a given RCS $\sigma_0$ at a given probability $p_{d0}$ with the probability of false alarm $p_{fa0}$. At the same time, characteristic pattern propagation factor and atmospheric loss factor are given as $F_0$ and $L_{a0}$, respectively.

With $p_{d0}$, $p_{fa0}$, Eq. (1) and (2), we can get the characteristic SNR $S_0$. Substituting $S_0$, $R_0$, $\sigma_0$, $F_0$, and $L_{a0}$ into Eq. (4) and solving for $v_0$ results in

$$v_0 = S_0 \frac{R_0^4 L_{\alpha 0}}{\sigma_0 F_0^4} \quad (5)$$

Substituting Eq. (5) into Eq. (4) results in

$$S = S_O \left(\frac{R_0}{R}\right)^4 \frac{\sigma}{\sigma_0} \frac{F^4 / L_\alpha}{F_0^4 / L_{\alpha 0}} \quad (6)$$

The signal-to-noise ratio here takes into account the object RCS (radar cross section), range, reflection clutter interference of land or sea, and atmospheric loss.

Given the location of aircraft and radar, $F$ and $L_a$. can be calculated [12], and $R$ can be calculated too. When the aircraft aspect with respect to the radar is known, σ can be obtained from the RCS Kriging approximation model. So $S$ can be solved form Eq. (6), and then we can solve the detection probability $p_d$ form Eq. (1) and (2).

## 3 Observability of Flight Route

As shown in Fig. 3, when the aircraft flies along the flight route represented by waypoint A-B, the radar will scan the aircraft several times. For the $i$-th scan of the aircraft, there will be a certain probability of detection $p_d(i)$ based on actual signal-to-noise ratio $S$, which can be determined from Eq. (6). Thus, $p_d(i)$ is generally a function of time.

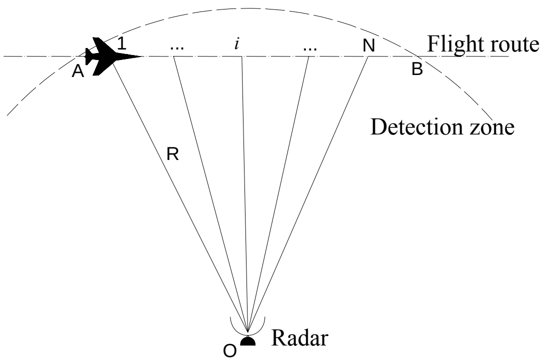


Fig. 3 Flight Route with Single Radar

In order to represent the observability of flight route, cumulative probability of detection $P_D$ is used here

$$P_D = 1 - \prod_{i=1}^{N} (1 - p_d(i)) \quad (7)$$

where $N$ is the number of scans. And $N$ is a function of radar scan periods $T$ and the time $t_{stay}$ during which the aircraft stays within the detection zone of the radar. $N$ is given by

$$N = \left\lfloor \frac{t_{stay}}{T} \right\rfloor \quad (8)$$

where ⌊ ⌋ is to choose the integer part of the result.

We assume that outside of the detection zones of the radars, which are shown with circular regions in the Fig. 3 with dashed lines, the probability of detection is zero.

We extend the single radar case to multiple radars case, as shown in Fig. 4.

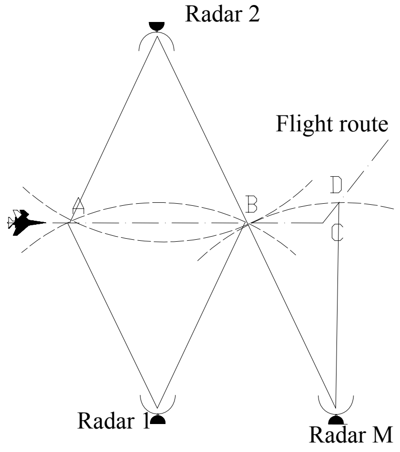


Fig. 4 Flight Route with Multiple Radars

Assume the scenario consists of $N$ radars, and the observability of flight route is represented by the global probability of detection

$$P_{D0}=1-\prod_{j=1}^{M}(1-P_D(j)) \tag{9}$$

where $P_{D0}$ is the global probability of detection of $M$ radars, and $P_D(j)$ is the cumulative probability of detection of the radar $j$.

Calculation of observability of flight route in the presence of multiple radars includes four steps:

1) Identify the bank and yaw angles of the aircraft at scan points.
2) Calculate the probability of detection for single scan at each scan point.
3) Compute the cumulative probabilities of detection for each radar.
4) Calculate the global observability of flight route.

## 4 Numerical Simulation

In order to investigate the proposed method, two examples are present in this section. We assume that pitch and bank angles are zero, so the calculation of the elevation and azimuth angles of aircraft with respect to radar is straightforward. The RCS data of the aircraft are given from 0 to 10 deg in elevation ($\theta$) and from 0 to 180 deg in azimuth ($\phi$). The resolution is 1 deg in elevation and 10 deg in azimuth. Fig.5 gives the Kriging approximation model of the aircraft RCS based on these data.

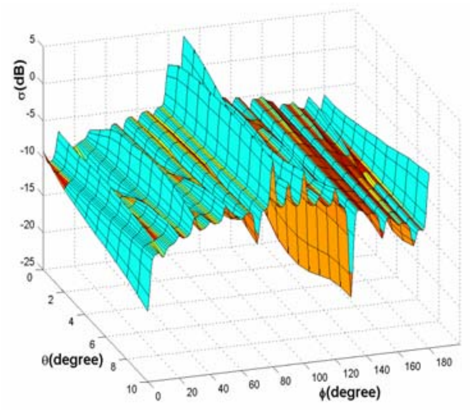


Fig. 5 The RCS Approximation Model using Kriging Method

As it is seen in Fig.3, the flight route is from waypoint $A$(-81.3km, 169km) to waypoint $B$(81.3km, 169km), and the radar location is $O$(0km, 0km, 0km). It is assumed that the types and basic system parameters of radar are known as shown in Table 1, then the elevation and azimuth angles can be calculated and RCS Kriging approximation model can be used.

Table 1 Types and Basic System Parameters of Radars

| Parameter | Value |
|---|---|
| Radar type | Early Warning Radar |
| Band | S |
| Frequency | 3 G Hz |
| Number of reference cells | 24 |
| Periods of scan | 12 $s$ |
| $R_0$ | 150 $Km$ |
| $\sigma_0$ | 1 m$^2$ |
| $p_{fa0}$ | $10^{-6}$ |
| $p_{d0}$ | 50% |
| $F_0^4/L_{a0}$ | 2.31 |
| Height of antenna $h_a$ | 30 m |

The first simulation gives the observability of flight route at different flight altitudes. In this simulation, the speed of the aircraft is fixed at 200 m/s. As it is seen in Fig. 6, the variation of the observability of flight route with respect to the flight altitude can be divided into three regions, the diffraction region, the interference region and the direct region.

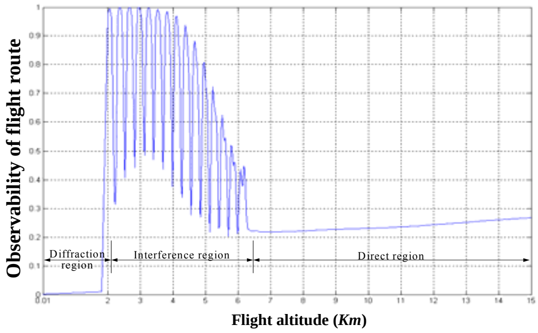


Fig. 6 Observability of Flight Route vs Flight Altitude

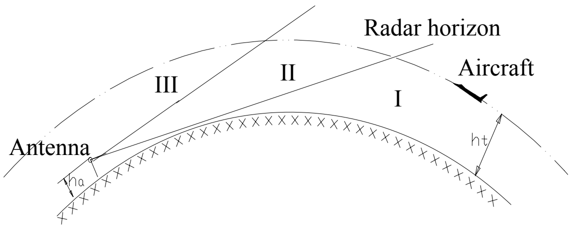


I: Diffraction region. II: Interference region. III: Direct region.

Fig. 7 Different Propagation Styles of Radar Electromagnetic Wave

As shown in Fig. 6 and 7, in the diffraction region, where $0<ht\leq 2$km, the observability of flight route is near to zero. This is because the aircraft is below the radar horizon; the radar signal can not propagate directly toward the aircraft. In the interference region, where $2\leq h\leq 7$km, the change of observability of flight route is relatively large. There are two kinds of signals in this region, one is the direct signal, and another is the signal reflections from the surface of the Earth. The reflected signal interferes with the direct signal first at the aircraft and then at the antenna. At some altitude, the interference strengthens the echo from the aircraft and cause a high observability of flight route; and at some altitude the observability of flight route is low. In the direct region, where $ht\geq 7$km, the atmospheric loss $La$ decreases as the altitude of the aircraft increases, so the observability of the flight route increases as $ht$ increases.

The second simulation gives the observability of flight route at different speeds. In this simulation, the altitude of the aircraft is fixed at 10km. As it is seen in Fig. 8, the observability of flight route monotonically decreases with increasing speed. This is caused by the decrease of the number of scans to the aircraft as the speed increases.

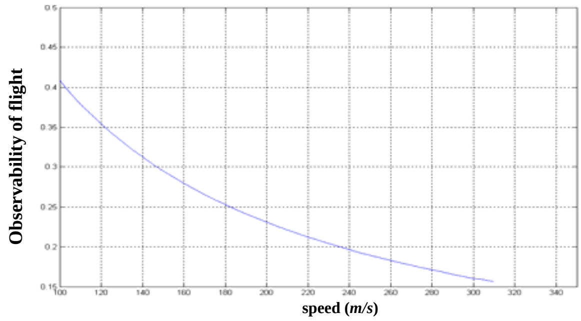


Fig. 8 Observability of Flight Route vs Speed

## 5 Conclusions and Future Work

This paper presented a method for calculating the observability of aircraft flight route in the presence of opponent radar systems. The simple numerical simulation shows that the method is reasonable and effective.

Through the proposed method, the observability of aircraft flight route can be quantified. Once the observability of aircraft flight route has been appropriately quantified, a variety of route planning algorithms are available for generating low observable aircraft flight routes. Future research will focus on determining which of these methods is the most effective.

## References


[1] David Arnaud, Brousseau Christian and Bourdillon Alain. Study of Flight Route Effects on Aircraft RCS Signature at VHF Frequencies by Means of Wire Grid Modes. *IEEE International Radar Conference*, pp 231-235, 2000.

[2] Norsell Martin. Flight Testing Radar Detection of the Saab 105 in Level Flight. *Journal of Aircraft*, Vol. 39, No. 5, pp 894-897, 2002.

[3] McFarland Michael B., Zachery Randy A. and Taylor Brian K.. Motion Planning for Reduced Observability of Autonomous Aerial Vehicles. *IEEE International Conference on Control Applications*, Hawaii, Vol. MP5, No. 3, pp 231-235, 1999.

[4] Moore Frank W.. Radar Cross-Section Reduction Via Route Planning and Intelligent Control. *IEEE Transactions on Control Systerm Technology*, Vol. 10, No. 5, pp 696-700, 2002.
[5] Norsell Martin. Radar Cross Section Constrains in Flight Path of Optimization. *41st Aerospace Sciences Meeting and Exhibit*, Reno, Vol. 105, 2003.
[6] Misovec K., Inanc T., Wohletz J. and Murray R. M.. Low-Observable Nonlinear Trajectory Generation for Unmanned Air Vehicles. *Conference on Decision and Control*, Hawaii, Vol. ThA02, No. 3, pp 3103-3110, 2003.
[7] Inanc Tamer, Misovec Kathy and Murray Richard M.. Nonlinear Trajectory Generation for Unmanned Air Vehicles with Multiple Radars. *43rd IEEE Conference on Decision and Control*, Atlantis, Vol. ThC05, No. 4, pp 3817-3822, 2004.
[8] Chaudhry Atif, Misovec Kathy and D'Andrea Raffaello. Low Observability Path Planning for an Unmanned Air Vehicle Using Mixed Integer Linear Programming. *43rd IEEE Conference on Decision and Control*, Atlantis, Vol. ThC05, No. 5, pp 3823-3829, 2004.
[9] Ball Robert E.. *The Fundamentals of Aircraft Combat Survivability Analysis and Design*, 2nd edition, American Institute of Aeronautics and Astronautics, Inc., 2003.
[10] Swerling P. and Peterman W. I.. Impact of Target RCS Fluctuations on Radar Measurement Accuracy. *IEEE Transactions*, Vol. AES-26, No. 4, pp 685-686, 1990.
[11] Gandhi P. P. and Kassam S. A.. Analysis of CFAR Processors in Nonhomogeneous Background. *IEEE Transactions on Aerospace and Electronic Systerm*, Vol. 24, No. 4, pp 427-445, 1988.
[12] Blake Lamont V. *Radar Range-Performance Analysis*. D. C. Heath and Company, 1980.